



Numerical investigation of rectangular thermal energy storage units with multiple phase change materials

S. Hoseinzadeh ^{a,*}, R. Ghasemiasl ^b, D. Havaei ^b, A.J. Chamkha ^{c,d}

^a Young Researchers and Elite Club, West Tehran Branch, Islamic Azad University, Tehran, Iran

^b Department of Mechanical Engineering, West Tehran Branch, Islamic Azad University, Tehran, Iran

^c Mechanical Engineering Department, Prince Sultan Endowment for Energy and Environment, Prince Mohammad Bin Fahd University, Al-Khobar 31952, Saudi Arabia

^d RAK Research and Innovation Center, American University of Ras Al Khaimah, United Arab Emirates

ARTICLE INFO

Article history:

Received 23 July 2018

Accepted 23 August 2018

Available online 25 August 2018

Keywords:

Enthalpy method

Latent heat thermal energy storage

Phase change material

Rectangular storage

ABSTRACT

Latent heat thermal storage (LHTS) using phase change materials (PCMs) is one of the efficient and useful technologies in conservation and retention of thermal energy. One of the main advantages of this technology is the utilization of such systems in cooling/heating applications where the air is the heat transfer fluid (HTF). Generally, the heat transfer rate in a LHTS unit and its efficiency depends on the difference between the melting temperature of the PCM and the HTF temperature. If a single PCM is used, the temperature difference between the PCM and the HTF along the flow direction will be decreased. This leads to a decrease in the heat transfer rate and efficiency. In this case, nearly a constant temperature difference between the PCM and the HTF can be maintained during phase change. Therefore, the heat transfer rate to/from the PCM is constant. This work presents a two-dimensional numerical investigation of the performance of the LHTS unit which is composed of several rectangular PCM slabs. The enthalpy method is used to solve the governing equations for the melting process in PCMs. The convective heat transfer inside the air channels is analyzed by solving the energy equation, which is coupled with the heat conduction equation in the PCM wall. The general equations of temperature and the local liquid fraction are discretized with the finite difference method and are solved by a fully implicit scheme. The effect of geometrical parameters of storage such as the PCM slab thickness and the length as well as the effect of air flow rate in the outlet air temperature of storage are investigated.

© 2018 Elsevier B.V. All rights reserved.

1. Introduction

Nowadays energy storage (ES) has been acquired to a position where it can have a significant result on modern technology. In special, ES is critically necessary to the accomplishment of any intermittent energy source in meeting demand. For instance, the need for storage in solar energy applications is severe, notably, meanwhile the solar energy is least available in winter [1,2].

In the present work, the melting process of the PCM and the heat transfer in HTF are studied numerically. The solution is carried out using a two-dimensional enthalpy method. The performance of a LHTS employing multiple PCMs is investigated. Fig. 1 illustrates the schematic diagram of the system. The system consists of several slabs of PCMs in which each slab contains two different PCMs. Air flows in channels between PCM slabs.

Zivkovic and Fujii performed a numerical analysis for isothermal phase change of the PCM encapsulated in rectangular and cylindrical containers based on the enthalpy method. Nedjar [3] stated an efficient

algorithm for solving non-linear heat transfer problems when the phase change takes place over a non-isothermal temperature range. Vakialtojar et al. [4] presented a semi-analytical model to evaluate the appearance of the storage systems in air conditioning and studied the impact of slab thickness on storage. Halawa et al. [5] improved a numerical analysis of freezing and melting of a PCM thermal storage unit (TSU) with a different wall temperature. Vyshak and Jilani [6] analyzed the total melting time of a PCM packed for three containers of various geometric configurations (cylindrical, rectangular, and cylindrical shell) having the same capacity and heat transfer surface area. Also, they determined that an increase in the inlet temperature of the HTF from a lower range of values results in a significant decrease in the energy storage time while the outcome of the inlet temperature of the HTF diminishes sharply at greater values. Chamkha et al. [7–10] proposed an analytical and numerical model of Single/Hybrid Nanoparticles PCM over a heated horizontal cylinder and MHD phase change heat transfer in an inclined enclosure. Saman et al. [11] employed a two-dimensional numerical method based on the enthalpy formulation and investigated the thermal appearance of a flat thermal storage unit. The outlet air temperatures and heat transfer rates predicted by this model were compared with experimental data, and showed close cooperation.

* Corresponding author.

E-mail address: Hoseinzadeh.siamak@gmail.com (S. Hoseinzadeh).

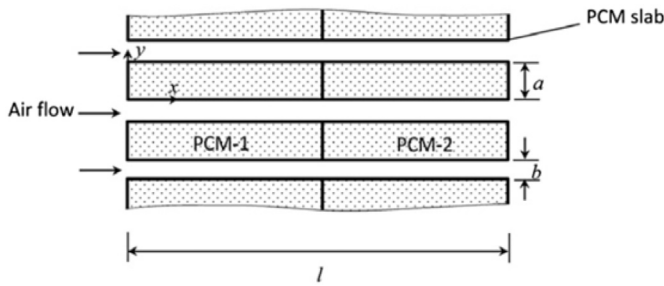


Fig. 1. Schematic diagram of the LHTS unit [16].

Halawa et al. [12] proposed a phase change processor algorithm to solve the phase change of the PCM in melting and solidification methods and also to determine the liquid fraction of the PCM node. Mosaffa et al. [13–15] presented energy, exergy and environmental analysis of air conditioning systems with thermal storage units. Hoseinzadeh et al. [16] studied a numerical analysis of performance of energy storage systems using two PCM with different nanoparticles.

2. Mathematical formulation

The solution of transient heat transfer problems involving melting or solidification generally referred as “phase change” or “moving boundary” problems is inherently difficult because the interface between the solid and liquid phases is moving as the latent heat is absorbed or released at the interface. As a result, the location of the solid-liquid interface is not known a priori and must follow as a part of the solution [17]. Numerical solution of unsteady two dimensional melting in a rectangular thermal energy storage unit containing slabs with multiple PCMs is studied. Voller [18,19] have shown that the enthalpy form of the energy equation can be written as:

$$\nabla \cdot (k \nabla T) = \rho \frac{\partial H}{\partial t} \quad (1)$$

The total enthalpy H can be divided into sensible and latent heat components. Therefore, an alternative form of Eq. (1) is as:

$$H = h + L \cdot f \quad (2)$$

where h is sensible heat which can be written as:

$$h = \int_{T_m}^T C dT \quad (3)$$

where T_m is the melting temperature of the PCM. In Eq. (2), f is the local liquid fraction and for isothermal phase change is Fig. 1.

Defined as:

$$f(T) = \begin{cases} 1 & \text{if } T > T_m \text{ (Liquid)} \\ 0 & \text{if } T < T_m \text{ (Solid)} \end{cases} \quad (4)$$

Substituting Eq. (4) into Eq. (1) gives:

$$\frac{\partial h}{\partial t} = \text{div} \left(\frac{k}{\rho} \text{grad } T \right) - L \frac{\partial f}{\partial t} \quad (5)$$

The governing energy equation for transient two-dimensional isothermal phase change of PCM with initial and boundary conditions is written as follows:

$$\frac{\partial h}{\partial t} = \frac{k}{\rho} \left(\frac{\partial^2 T}{\partial x^2} + \frac{\partial^2 T}{\partial y^2} \right) - L \frac{\partial f}{\partial t} \quad (6)$$

$$T(x, y, 0) = T_i \quad (7)$$

$$k \frac{\partial T(x, 0, t)}{\partial y} = -k \frac{\partial T(x, a, t)}{\partial y} = h_c(T_w - T_f) \quad (8)$$

$$\frac{\partial T(0, y, t)}{\partial x} = -k \frac{\partial T(l, y, t)}{\partial x} = 0 \quad (9)$$

The governing energy equation with initial and boundary conditions for incompressible and laminar flow with no viscous dissipation are written as [20,21]:

$$\frac{\partial T_f}{\partial t} + u \frac{\partial T_f}{\partial x} = \frac{k_f}{\rho_f c_f} \left(\frac{\partial^2 T_f}{\partial y^2} \right) \quad (10)$$

$$T_f(x, y, 0) = T_i \quad (11)$$

$$k_f \frac{\partial T_f(x, 0, t)}{\partial y} = -k_f \frac{\partial T(x, -b, t)}{\partial y} = h_c(T_w - T_f) \quad (12)$$

$$T_f(0, y, t) = T_{inlet} \quad (13)$$

The convective heat transfer coefficient is defined as:

$$h_c(x) = - \frac{k}{T_{f,b}(x) - T_w(x)} \cdot \frac{\partial T(x, y)}{\partial y} \quad (14)$$

where $T_{f,b}$ is the fluid bulk temperature defined as:

$$T_{f,b} = \frac{\int u(y) T_f(x, y) dy}{\int u(y) dy} \quad (15)$$

Therefore, the local Nusselt number will be as:

$$Nu(x) = \frac{h_c(x) D_h}{k_f} \quad (16)$$

3. Numerical solution

The domain of solution is consisted of the half part of one PCM slab and half part of the air gap where partitioned in equidistant nodes. The control volume associated with each node has thicknesses Δx and Δy in the x - and y -directions, respectively. The central difference discretization of temperature field for any internal node (i, j) can be written as:

Any internal node (i, j) can be written as:

$$\frac{\partial h_{i,j}}{\partial t} = \frac{k}{\rho(\Delta x)^2} (T_{i-1,j} - 2T_{i,j} + T_{i+1,j}) + \frac{k}{\rho(\Delta y)^2} (T_{i,j-1} - 2T_{i,j} + T_{i,j+1}) - L \frac{\partial f_{i,j}}{\partial t} \quad (17)$$

For isothermal phase change the temperature of a given control volume, remains constant at melting/freezing temperature. Consider the situation that the PCM in the control volume (i, j) is fully solid or fully liquid. In this state, with considering Eq. (4), the value of f will be equal to 0 or 1. From the definition of the sensible enthalpy $(\partial h_{i,j}/\partial t = c \partial T_{i,j}/\partial t)$ with substituting in Eq. (17), the heat diffusion equation is defined as:

$$\frac{\partial T_{i,j}}{\partial t} = \frac{k}{\rho c(\Delta x)^2} (T_{i-1,j} - 2T_{i,j} + T_{i+1,j}) + \frac{k}{\rho c(\Delta y)^2} (T_{i,j-1} - 2T_{i,j} + T_{i,j+1}) \quad (18)$$

Backward differencing of the temperature term at the left side and using a fully implicit scheme with considering the thermal

Table 1
Thermal properties of the selected PCM [21].

Property	CaCl ₂ ·6H ₂ O	RT25
Density, ρ (kg m ⁻³)	1710 (solid) 1530 (liquid)	785 (solid) 749 (liquid)
Heat capacity, c (J kg ⁻¹ °C ⁻¹)	1400 (solid) 2200 (liquid)	1410 (solid) 1800 (liquid)
Thermal conductivity, k (W m ⁻¹ K ⁻¹)	1.09 (solid) 0.53 (liquid)	0.19 (solid) 0.18 (liquid)
Latent heat of fusion, L (J kg ⁻¹)	187,000	232,000
Melting temperature, T _m (°C)	29	26.6

diffusivity definition ($\alpha = k/\rho c$), the following discretized equation results:

$$T_{i,j} = T_{i,j}^{old} \frac{\alpha \Delta t}{(\Delta x)^2} (T_{i-1,j} - 2T_{i,j} + T_{i+1,j}) + \frac{\alpha \Delta t}{(\Delta y)^2} (T_{i,j-1} - 2T_{i,j} + T_{i,j+1}) \quad (19)$$

When melting occurs within the control volume (i,j), the liquid fraction f lies in the interval [0, 1]. In this case, $T_{i,j} = T_m$ and therefore $\partial h_{i,j} / \partial t = 0$. So, the fully implicit finite difference equation of Eq. (17) for an internal control volume can be written as:

$$f_{i,j} = f_{i,j}^{old} \frac{k \Delta t}{\rho L (\Delta x)^2} (T_{i-1,j} - 2T_{i,j} + T_{i+1,j}) + \frac{k \Delta t}{\rho L (\Delta y)^2} (T_{i,j-1} - 2T_{i,j} + T_{i,j+1}) \quad (20)$$

3.1. Start and end of melting process

For a given time step, if $T_{i,j} \geq T_m$ while $T_{i,j}^{old} < T_m$, it indicates that within this time step, the control volume, begins with melting, and if $f_{i,j} \geq 1$ while $f_{i,j}^{old} < 1$, it indicates that, the control volume has melted completely.

4. Results and discussion

For air conditioning systems PCMs have to have a melting temperature within the range of human comfort conditions. The PCMs considered

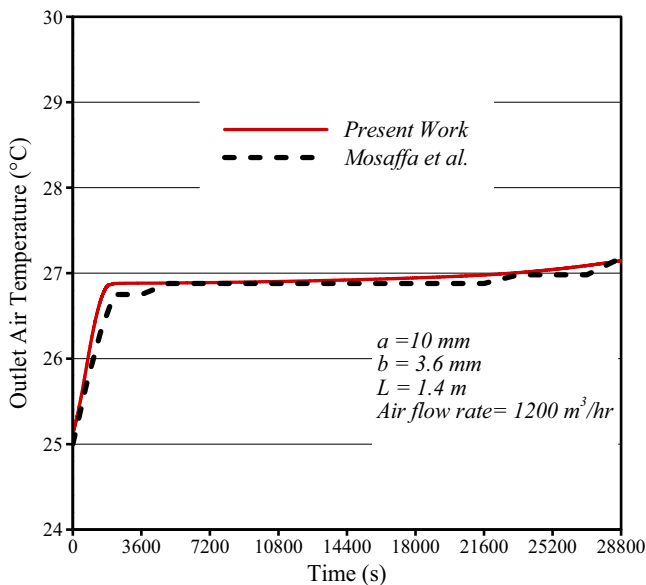


Fig. 2. Comparison of outlet air temperature time history by the effective heat capacity method and enthalpy method.

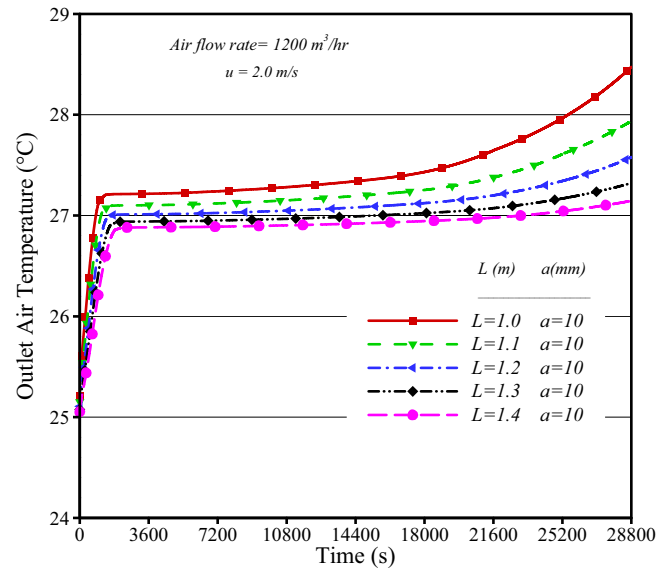


Fig. 3. The effect of PCM slab length on the outlet air temperature.

in this investigation are calcium chloride hexahydrate (CaCl₂·6H₂O) and RT25. They are packed in the system in decreasing order of their melting points. Thermal properties of the PCMs are listed in Table 1.

4.1. Model validation

To show the validation of the present method, results that are obtained with present method are compared with the results reported by articles [17–22]. We used the effective heat capacity method as the numerical method and modelling was carried out using COMSOL Multiphysics and MATLAB [23–30]. Fig. 2 shows the outlet air temperature time history with similar storage dimensions. The inlet air temperature and initial temperature of the PCMs are 36 °C and 25 °C, respectively. The figure shows a great agreement between the contemporary model and those stated.

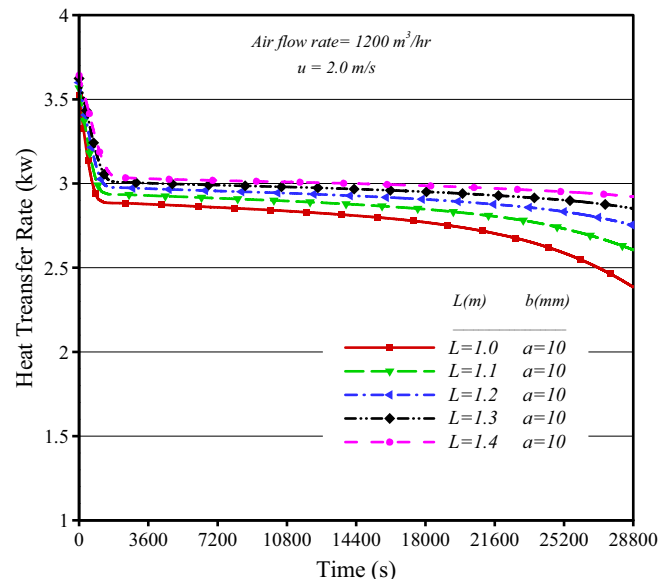


Fig. 4. The effect of PCM slab length on the heat transfer rate.

Table 2
Storage dimensions used in the calculations.

Thickness of PCM slabs, a	10 mm
Thickness of air channels, b	4 mm
Length of PCM slabs, l	1.3 m
Height of storage	0.5 m
Width of storage	1.12 m
Air flow rate, \dot{V}	$1200 \text{ m}^3 \text{ h}^{-1}$ ($u = 2 \text{ m s}^{-1}$)

4.2. Multiple PCMs thermal storage units

The thermal storage dimensions presented in Table 1 are used for the calculations. The Comparison of outlet air temperature time history by the effective heat capacity method and enthalpy method is shown in Fig. 2.

Fig. 3 shows the effect of PCM slab length on the outlet air temperature. Air temperature increases quickly to the initial temperature of the PCMs in a short time. In the result of the heat transfer between the air flow and the PCMs wall, the temperature of the surface of the PCMs reaches to the melting temperature and the outlet air temperature rises slowly because a large portion of the heat is used to melt the PCMs. The results show that an increase in the length of the PCMs causes a decrease in outlet air temperature.

Fig. 4 shows the effect of the length of the PCM slabs on the heat transfer rate during the melting process. When the outlet air temperature rises, due to the decrease in the temperature difference between the air and the PCM, the heat transfer rate decreases sharply. When the temperature of the boundary points of the PCM slabs reaches to the melting point, the heat transfer occurs with a constant rate. This is reflected in a very slow increase in the air outlet temperature. The results show that increasing the PCM slabs causes increases in the heat transfer rate (Table 2).

Fig. 5 illustrates the effect of the PCM slab thickness on the outlet air temperature when the mass of the PCM remains constant. Reducing the slab thickness with a constant mass of the PCM causes an increase in the heat transfer area because the number of slabs will be increase. Therefore, the heat transfer rate is increased and the outlet air temperature is decreased.

Figs. 5 and 6 shows the outcome of the air channel thickness on the outlet air temperature. For a given slab thickness, as the air gap is

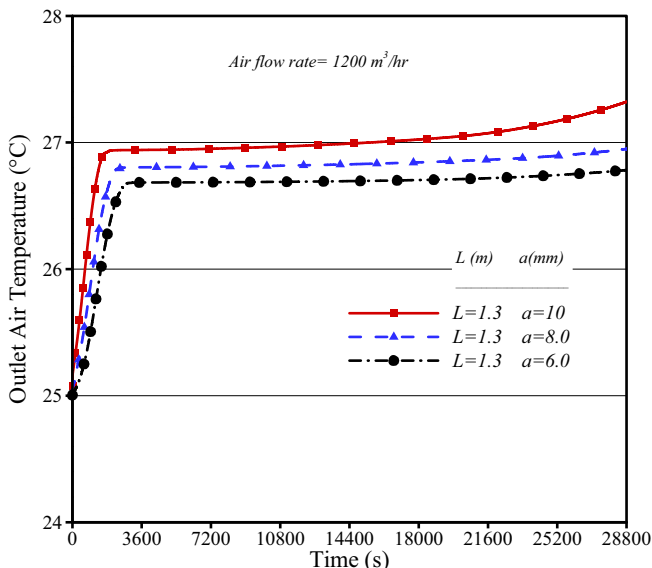


Fig. 5. The effect of PCM slab thickness on the outlet air temperature.

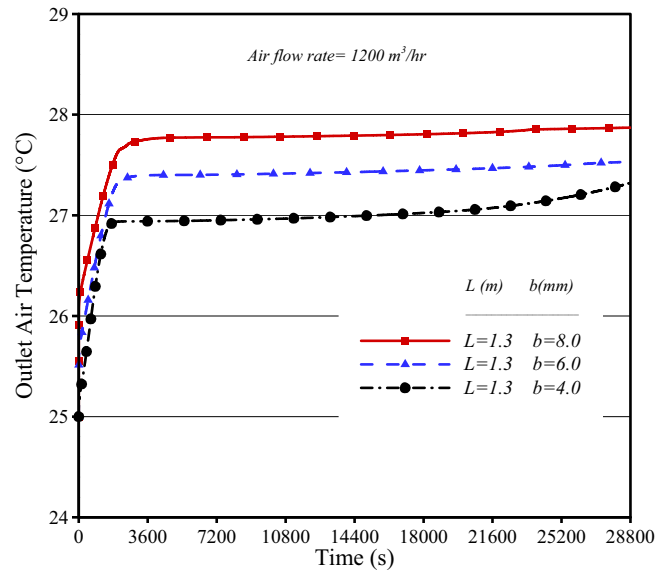


Fig. 6. The effect of air channel thickness on the outlet air temperature.

decreased, the Reynolds number remains constant (the air velocity is increased, but the hydraulic diameter is reduced) and accordingly, Nusselt does not vary. Nevertheless, the convective heat transfer coefficient is increased as a result of the decrease of the hydraulic diameter.

Fig. 7 shows the effect of the air flow rate on the outlet air temperature. Increasing the air flow rate and the velocity increases the Reynolds number. Therefore, the Nusselt number and the heat transfer coefficient are increased and the heat transfer rate and the outlet air temperature are raised. It can be seen that to keep the outlet air temperature below the 28°C for about 8 h, the maximum air flow rate for the system is $1450 \text{ m}^3 \text{ h}^{-1}$.

Fig. 8 shows the predicted time of the melting of the multiple PCMs encapsulated in the LHES with different inlet air velocities. The liquid fraction of the PCM indicated how much of a PCM in the storage is molted. As shown in Fig. 8, an increase in the air velocity results in increases in the Reynolds and Nusselt numbers and the heat transfer rate and therefore, the fraction of molten PCM increases.

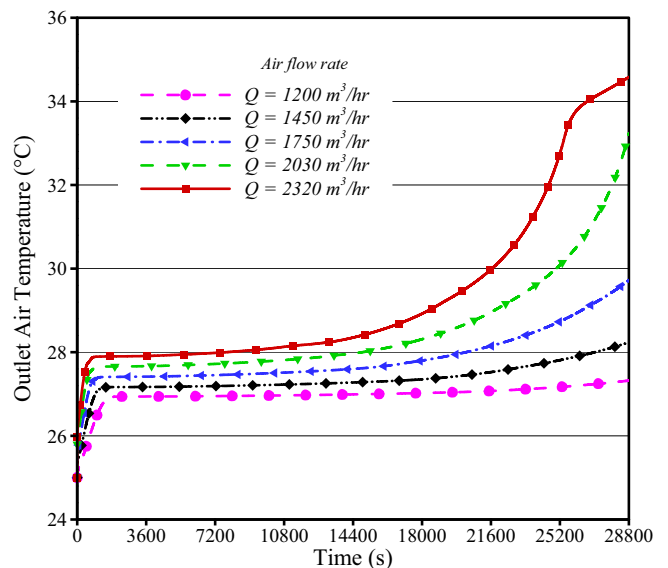


Fig. 7. The effect of air flow rate on the outlet air temperature.

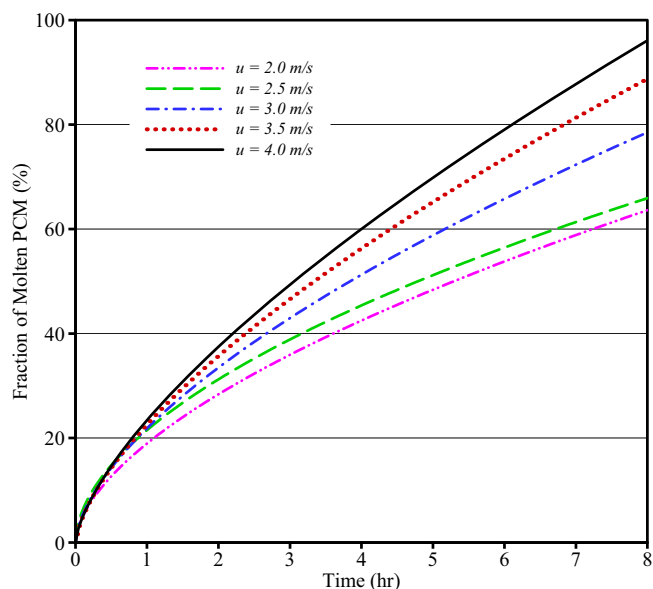


Fig. 8. The effect of air velocity on the fraction of molten PCM.

5. Conclusion

A numerical investigation based on the enthalpy method is developed for the melting process of multiple PCMs encapsulated in a rectangular container. Air is used as the heat transfer fluid and $\text{CaCl}_2 \cdot 6\text{H}_2\text{O}$ and RT25 as the PCMs. The results show that a better performance can be obtained by using longer and thinner PCM slabs. Also, by using a smaller air channel thickness, the outlet air temperature decreases. By using thinner PCM slabs, the number of PCM containers increases. Therefore, the total volume of the storage system increases and this leads to a higher pressure drop across the storage system. A comparison between different air flow rates and their influence on the outlet air temperature and a fraction of the molten PCM is shown. The results show that when the flow rate is increased, the fraction of the molten PCM and the outlet air temperature are increased.

Conflict of interest statement

We declare that we have no financial or personal relationships with other people or organizations that could inappropriately influence (bias) our work.

Nomenclature

a	thickness of PCM slab, m
b	thickness of air channel, m
c	specific heat of PCM, $\text{J kg}^{-1}\text{K}^{-1}$
c_f	specific heat of air, $\text{J kg}^{-1}\text{K}^{-1}$
D_h	hydraulic diameter, m
f	liquid fraction
H	total enthalpy, J kg^{-1}
h	sensible enthalpy, J kg^{-1}
h_c	convective heat transfer coefficient, $\text{W m}^{-2}\text{K}^{-1}$
k	thermal conductivity of PCM, $\text{W m}^{-1}\text{K}^{-1}$
k_f	thermal conductivity of air, $\text{W m}^{-1}\text{K}^{-1}$
L	latent heat of fusion, J kg^{-1}
l	length of storage, m
$Nu(x)$	local Nusselt number
T	PCM temperature, $^{\circ}\text{C}$
T_m	melting temperature, $^{\circ}\text{C}$
T_f	fluid temperature, $^{\circ}\text{C}$
$T_{f,b}$	fluid bulk temperature, $^{\circ}\text{C}$

T_w	wall temperature, $^{\circ}\text{C}$
T_i	initial temperature, $^{\circ}\text{C}$
T_{inlet}	inlet temperature of air, $^{\circ}\text{C}$
t	time, s
u	velocity of air, m s^{-1}
\dot{V}	volumetric flow rate, $\text{m}^3\text{ h}^{-1}$
α	thermal diffusivity of PCM, $\text{m}^2\text{ s}^{-1}$
ρ	density of PCM, kg m^{-3}
ρ_f	density of air, kg m^{-3}

References

- [1] I. Dincer, M.A. Rosen, *Thermal Energy Storage Systems and Applications*, second ed. John Wiley & Sons, Chichester, 2011.
- [2] B. Zivkovic, I. Fujii, An analysis of isothermal phase change of phase change material within rectangular and cylindrical containers, *Sol. Energy* 70 (2001) 51–61.
- [3] B. Nedjar, An enthalpy-based finite element method for nonlinear heat problems involving phase change, *Comput. Struct.* 80 (2002) 9–21.
- [4] S.M. Vakilaltojjar, W. Saman, Analysis and modelling of a phase change storage system for air conditioning applications, *Appl. Therm. Eng.* 21 (2001) 249–263.
- [5] E. Halawa, F. Bruno, W. Saman, Numerical analysis of a PCM thermal storage system with varying wall temperature, *Energy Convers. Manag.* 46 (2005) 2592–2604.
- [6] N.R. Vyshak, G. Jilani, Numerical analysis of latent heat thermal energy storage system, *Energy Convers. Manag.* 48 (2007) 2161–2168.
- [7] A.J. Chamkha, A. Doostanidezfouli, E. Izadpanahi, M. Ghalambaz, Phase-change heat transfer of single/hybrid nanoparticles-enhanced phase-change materials over a heated horizontal cylinder confined in a square cavity, *Adv. Powder Technol.* 28 (2017) 385–397.
- [8] M. Ghalambaz, A.D. Dezfouli, H. Zargartalebi, A.J. Chamkha, MHD phase change heat transfer in an inclined enclosure: effect of magnetic field and cavity inclination, *Numer. Heat Transfer, Part A* 71 (2017) 91–109.
- [9] M. Ghalambaz, A. Doostanidezfouli, E. Izadpanahi, A.J. Chamkha, Phase-change heat transfer in a cavity heated from below: the effect of utilizing single or hybrid nanoparticles as additives, *J. Taiwan Inst. Chem. Eng.* 72 (2017) 104–115.
- [10] M. Ghalambaz, A. Doostani, A.J. Chamkha, M. Ismeal, Melting of nanoparticles-enhanced phase-change materials in an enclosure: effect of hybrid nanoparticles, *Int. J. Mech. Sci.* 134 (2017) 85–97.
- [11] W. Saman, F. Bruno, E. Halawa, Thermal performance of PCM thermal storage unit for a roof integrated solar heating system, *Sol. Energy* 78 (2005) 341–349.
- [12] E. Halawa, W. Saman, F. Bruno, A phase change processor method for solving a one-dimensional phase change problem with convection boundary, *Renew. Energy* 35 (2010) 1688–1695.
- [13] A.H. Mosaffa, L. Garousi Farshi, C.A. Infante Ferreira, M.A. Rosen, Energy and exergy evaluation of a multiple-PCM thermal storage unit for free cooling applications, *Renew. Energy* 68 (2014) 452–458.
- [14] A.H. Mosaffa, L. Garousi Farshi, C.A. Infante Ferreira, M.A. Rosen, Advanced exergy analysis of an air conditioning system incorporating thermal energy storage, *Energy* 77 (2014) 945–952.
- [15] A.H. Mosaffa, L. Garousi Farshi, Exergoeconomic and environmental analyses of an air conditioning system using thermal energy storage, *Appl. Energy* 162 (2016) 515–526.
- [16] R. Ghasemiasl, S. Hoseinzadeh, M.A. Javadi, Numerical analysis of performance of energy storage systems using two phase-change material with nanoparticles, *AIAA J.* 32 (2018) 440, <https://doi.org/10.2514/1.T5252>.
- [17] M.N. Özışık, *Heat Conduction*, second ed. Wiley, New York, 1993.
- [18] V.R. Voller, Implicit finite-difference solutions of the enthalpy formulation of Stefan problems, *IMA J. Numer. Anal.* 5 (1985) 201–214.
- [19] V.R. Voller, Fast implicit finite-difference method for the analysis of phase change problems, *Numer. Heat Transfer Part B* 17 (1990) 155–169.
- [20] H. El Qarnia, Theoretical study of transient response of a rectangular latent heat thermal energy storage system with conjugate forced convection, *Energy Convers. Manag.* 45 (2004) 1537–1551.
- [21] F. Agyenim, N. Hewitt, P. Eames, M. Smyth, A review of materials, heat transfer and phase change problem formulation for latent heat thermal energy storage systems (LHTES), *Renew. Sust. Energ.* 14 (2010) 615–628.
- [22] A.H. Mosaffa, C.A. Infante Ferreira, F. Talati, M.A. Rosen, Thermal performance of a multiple PCM thermal storage unit for free cooling, *Energy Convers. Manag.* 67 (2013) 1–7.
- [23] S. Hoseinzadeh, R.J. Azadi, Renewable sustainable energy, simulation and optimization of a solar-assisted heating and cooling system for a house in Northern of Iran, *Am. Inst. Phys.* 9 (4) (2017), 045101.
- [24] M.E. Yousef Nezhad, S. Hoseinzadeh, Mathematical simulation and optimization of a solar water heater for an aviculture unit using MATLAB/SIMULINK, *J. Renew. Sust. Energ., Am. Inst. Phys.* 9 (6) (2017), 063702.
- [25] A. Ghasemi, M. Dardel, M.H. Ghasemi, Collective effect of fluid's colioris force and nano-scale's parameter on instability pattern and vibration characteristic of fluid-conveying carbon nanotubes, *J. Press. Vessel. Technol.* 137 (3).
- [26] A. Ghasemi, M. Dardel, M.H., Ghasemi, Control of the non-linear static deflection experienced by a fluid-carrying double-walled carbon nanotube using an external distributed load, *Proc. Inst. Mech. Eng. Part N J. Nanoeng. Nanosyst.* 226 (1012) 181–190.

- [27] S. Hoseinzadeh, S.A.R. Sahebi, R. Ghasemiasl, et al., Effect of Al₂O₃/water nanofluid on thermosyphon thermal performance, *Eur. Phys. J. Plus* 132 (2017) 197, <https://doi.org/10.1140/epjp/i2017-11455-3>.
- [28] A. Yari, S. Hosseinzadeh, A.A. Golneshan, R. Ghasemiasl, Numerical simulation for thermal design of a gas water heater with turbulent combined convection, *ASME Proceedings Symposium on Applications in CFD*, ASME, 2015, AJKFluids2015-3305: V001T03A007.
- [29] M. Eftari, S. Hoseinzadeh, H.J. Javaniyan, M.F.T. Emadi, Analytical solution for free convection non-newtonian flow between two vertical sheets, *World Appl. Sci. J.* 16 (2012) (Special Issue of Applied Math).
- [30] A. Bahrami, S. Hosseinzadeh, R. Ghasemiasl, Solution of non-fourier temperature field in a hollow sphere under harmonic boundary condition, *Appl. Mech. Mater.* 772 (2015) 197.